PASSIVITY-BASED DYNAMIC BIPEDAL WALKING WITH TERRAIN ADAPTABILITY

Dynamics, Control and Robotic Applications

Qining Wang, Long Wang, Jinying Zhu, Yan Huang and Guangming Xie
Intelligent Control Laboratory, College of Engineering, Peking University, Beijing 100871, China

Keywords: Passive dynamic walking, Bipedal robots, Terrain adaptability, Modeling.

Abstract: This paper presents an approach for passivity-based bipedal robots to achieve stable walking on uneven terrain. A powered two-dimensional seven-link walking model with flat feet and compliant ankles has been proposed to analyze and simulate the walking dynamics. We further describe an optimization based control method, which uses optimized hip actuation and ankle compliance as control parameters of bipedal walking. Satisfactory results of simulations and real robot experiments show that the passivity-based walker can achieve stable bipedal walking with larger ground disturbance by the proposed method in view of stability and efficiency.

1 INTRODUCTION

Stability guaranteed dynamic bipedal walking is one of the keys but also one of the more challenging components of humanoid robot design. Several actively controlled bipedal robots are able to deal with such dynamic stability when walk on irregular surface (Yamaguchi and Takanishi, 1997), step over obstacles (Guan et al., 2006), climb stairs (Michel et al., 2007), even if achieve bipedal running (Honda Motor, 2005). However, to increase the autonomy of the robot, the locomotion efficiency, which is far from that of human motion, has to be improved.

As one of the possible explanations for the efficiency of the human gait, passive dynamic walking (McGeer, 1990) showed that a mechanism with two legs can be constructed so as to descend a gentle slope with no actuation and no active control. Several studies reported that these kinds of walking machines work with reasonable stability over a range of slopes (e.g. (McGeer, 1990), (Collins et al. 2001)) and on level ground with kinds of actuation added (e.g. (Collins et al. 2005), (Wisse et al., 2007)) show a remarkable resemblance to the human gait. In spite of having high energetic efficiency, passivity-based walkers have limits to achieve adaptive locomotion on rough terrain, which is one of the most important advantages of the legged robots. In addition, these walkers are sensitive to the initial conditions of walking.

To overcome such disadvantages, several studies proposed quasi-passive dynamic walking methods, which implement simple control schemes and actuators supplementarily to handle ground disturbances. For example, (Schuitema et al., 2005) described a reinforcement learning based controller and showed that the walker with such controller can maximally overcome $-10mm$ ground disturbance. (Tedrake et al., 2004) presented a robot with a minimal number of degrees of freedom which is still capable of stable dynamic walking even on level ground and even up a small slope. (Wang et al., 2006) designed a learning controller for a two-dimensional biped model with two rigid legs and curved feet to walk on uneven surface that monotonically increases from $12mm$ to $40mm$ with a $2mm$ interval. In these studies, passivity-based walkers are often modeled with point feet or round feet. And the control parameter only includes hip actuation. None of them analyzed the stability or adaptability in quasi-passive dynamic walking with flat feet and ankle joint compliance which is more close to human motion. In fact, flat feet can offer the advantage of distributing the energy loss per step over two collisions, at the heel and at the toe (Kwan and Hubbard, 2007), (Ruina et al., 2005). Moreover, experiments on human subjects and robot prototypes revealed that the tendon of the muscle in ankle joint is one mechanism that favors locomotor economy (Fukunaga et al., 2001), (Wang et al., 2007). It is predictable that by controlling and optimizing the hip actuation and ankle compliance, the passivity-based bipedal walker may achieve adaptive bipedal locomotion with larger disturbance on uneven terrain.

Wang Q., Wang L., Zhu J., Huang Y. and Xie G. (2009).
PASSIVITY-BASED DYNAMIC BIPEDALWALKING WITH TERRAIN ADAPTABILITY - Dynamics, Control and Robotic Applications.
In *Proceedings of the 6th International Conference on Informatics in Control, Automation and Robotics - Robotics and Automation*, pages 29-36
DOI: 10.5220/0002184200290036

In this paper, we investigate how to control passivity-based bipedal walkers to achieve stable walking with terrain adaptability. A powered two-dimensional seven-link walking model with flat feet and ankle compliance has been proposed to analyze and simulate the walking dynamics. We hypothesized that the nervous system that controls human locomotion may use optimized hip actuation and joint compliance to achieve stable bipedal walking on irregular terrain. Actually, hip actuation will cause the walker to change locomotive patterns. Furthermore, we use both simulations and real robot prototype to explore the performance of the passivity-based walkers when walk on uneven terrain by utilizing a biologically inspired optimization based controller, which is adaptive and capable of selecting proper hip actuation and ankle compliance in view of walking stability and efficiency.

This paper is organized as follows. Section II describes the walking dynamics of the biped with flat feet and ankle compliance. In Section III, we present the optimization based walking control method. In section IV, experimental results of stable locomotion with terrain adaptability are shown. We conclude in Section V.

2 PASSIVITY-BASED BIPEDAL WALKER

Our model extended the Simplest Walking Model (Garcia et al., 1998) with the addition of hip joint actuation, upper body, flat feet and linear spring based compliance on ankle joints, aiming for adaptive bipedal locomotion with optimization based controller. The model consists of an upper body (point mass added stick) that rotates around the hip joint, a point mass representing the pelvis, two legs with knee joints and ankle joints, and two mass added flat feet (see Fig. 1).

The mass of each leg is simplified as point masses added on the Center of Mass (CoM) of the shank and the thigh respectively. Similar to (Wisse et al., 2004), a kinematic coupling has been used in the proposed model to keep the body midway between the two legs. In addition, our model added compliance in ankle joints. Specifically, the ankle joints are modeled as passive joints that are constrained by linear springs. The model is implemented in MATLAB, using the parameter values shown in Table 1, which are derived from the mechanical prototype.

The passive walker travels forward on level ground. The stance leg keeps contact with the ground while the swing leg pivots about the constraint hip.

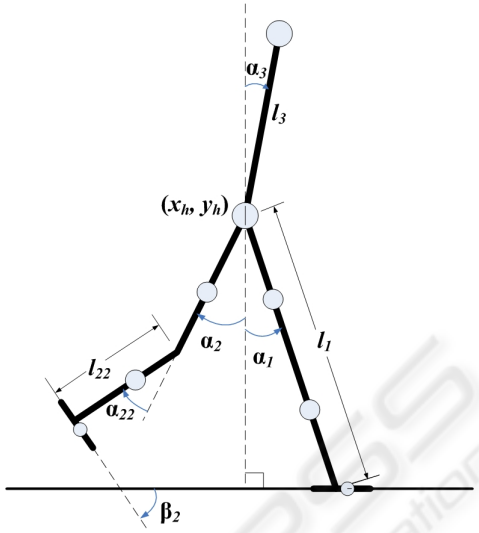

Figure 1: Two-dimensional seven-link passive dynamic walking model. Mechanical energy consumption of level ground walking is compensated by applying a hip torque. The global coordinates of the hip joint is notated as (x_h, y_h). α_1 and α_2 are the angles between each leg and the vertical axis in sagittal plane respectively. The knee joints and ankle joints are all passive joints. To simulate human ankle compliance, the ankle joints of the model are constrained by linear springs.

Table 1: Default Parameter Values for the dynamic walking model and the following simulations.

Parameter	Description	Value
m_1, m_2	leg mass	$1.12kg$
m_3	upper body mass	$0.81kg$
m_4	hip mass	$15.03kg$
m_{1t}, m_{2t}	thigh mass	$0.56kg$
m_{1s}, m_{2s}	shank mass	$0.56kg$
m_{f1}, m_{f2}	foot mass	$2.05kg$
l_1, l_2	leg length	$0.7m$
l_{11}, l_{22}	shank length	$0.35m$
l_{f1}, l_{f2}	foot length	$0.15m$
l_b	upper body length	$0.5m$
l_w	body width	$0.15m$
c_b	CoM of upper body	$0.2m$
c_1, c_2	CoM of leg	$0.2m$
c_{11}, c_{22}	CoM of shank	$0.2m$
k	ankle stiffness	$8.65Nm/rad$
P	hip torque	$0.38Nm$

To compensate the mechanical energy consumption, similar to (Kuo, 2002), we added a hip torque P between the swing leg and the stance leg. When the flat foot strikes the ground, there are two impulses, "heel-strike" and "foot-strike", representative of the initial impact of the heel and the following impact as the

whole foot contacts the ground.

The walking model can be defined by the rectangular coordinates x which can be described by the x-coordinates and y-coordinates of the mass points and the corresponding angles. The walker can also be described by the generalized coordinates q. The springs on the ankles constrain the foot vertical to the shank when no heel-strike or foot-strike has occurred.

2.1 Constraint Equations

The constraint equations ξ_1 and ξ_2 used to detect heel contact with ground are defined as follows:

$$\begin{aligned} \xi_1 &= \begin{bmatrix} x_h + l_1 \sin\alpha_1 - l_{f1}\cos\alpha_1 - x_{f1} \\ y_h - l_1\cos\alpha_1 - l_{f1}\sin\alpha_1 \end{bmatrix} \\ \xi_2 &= \begin{bmatrix} x_h + l_2 \sin\alpha_2 - l_{f2}\cos\alpha_2 - x_{f2} \\ y_h - l_2\cos\alpha_2 - l_{f2}\sin\alpha_2 \end{bmatrix} \end{aligned} \quad (1)$$

where x_{f1} and x_{f1} are the global x-coordinates of the latest strike. When the flat foot completely contacts the ground, the constraint equations ξ_3 and ξ_4 used to maintain foot contact with ground are defined as follows:

$$\begin{aligned} \xi_3 &= \begin{bmatrix} x_h + l_1 \sin\alpha_1 - x_{f1} \\ y_h - l_1\cos\alpha_1 \end{bmatrix} \\ \xi_4 &= \begin{bmatrix} x_h + l_2 \sin\alpha_2 - x_{f2} \\ y_h - l_2\cos\alpha_2 \end{bmatrix} \end{aligned} \quad (2)$$

If only the heel contacts the ground, the constraint equations ξ_5 and ξ_6 during the period before foot-strike are defined as follows:

$$\begin{aligned} \xi_5 &= (x_h + l_1\sin\alpha_1 - x_{f1})^2 + (y_h - l_1\cos\alpha_1)^2 - l_{f1}^2 \\ \xi_6 &= (x_h + l_2\sin\alpha_2 - x_2)^2 + (y_h - l_2\cos\alpha_2)^2 - l_{f2}^2 \end{aligned} \quad (3)$$

Note that ξ_5 and ξ_6 are similar to constraining the ankle joint that connects shank and foot to move in a circular orbit with heel as the center and distance between heel and ankle joint as the radius.

Similar to (Wisse et al., 2004), a reduced mass matrix M_r is introduced, which is defined as follows:

$$[M_r] = [T]^T [M_g] [T] \quad (4)$$

where the Jacobian $T = \frac{\partial x}{\partial q}$. Here x is the global coordinates of the six pointmasses (stance shank with foot, swing shank with foot, hip, stance thigh, swing thigh, body), while M_g is the mass matrix in global coordinates. Matrix Ξ_i transfers the independent generalized coordinates q into the constraint equation ξ_i, where $i = 1, 2, \ldots, 6$

$$\Xi_i = \frac{d\xi_i}{dq} \quad (5)$$

Consequently, matrix $\tilde{\Xi}_i$ is defined as follows:

$$\tilde{\Xi}_i = \frac{\partial(\Xi_i \dot{q})}{\partial q}\dot{q} \quad (6)$$

2.2 Single Support Phase

Suppose that leg 1 (l_1) is the stance leg, while leg 2 (l_2) is the swing leg. In the beginning of the single support phase, the knee joint is locked (keep the shank and the thigh in a straight line). The Equation of Motion (EoM) is described as follows:

$$\begin{bmatrix} M_r & \Xi_3^T \\ \Xi_3 & 0 \end{bmatrix} \begin{bmatrix} \ddot{q} \\ F_c \end{bmatrix} = \begin{bmatrix} F_r \\ -\tilde{\Xi}_3 \end{bmatrix} \quad (7)$$

where F_r is the external force, while F_c is the foot contact force. Here, the external force F_r is used to compensate the mechanical energy consumption of level ground walking, which defined as follows:

$$\{F_r\} = [T]^T (\{F\} - [M_g]\{\ddot{x}\})$$

where F is the external force in global coordinates, including gravity, hip actuation, and torque in compliant ankle joints. Then when the swing leg is swung forward, the knee joint releases the shank.

2.3 Heel-strike Phase

In this phase, leg 1 (l_1) is still the stance leg, while leg 2 (l_2) is the swing leg. The heel contacts the ground (heel-strike occurs). The EoM of the model changes to:

$$\begin{bmatrix} M_r & \Xi_6^T \\ \Xi_6 & 0 \end{bmatrix} \begin{bmatrix} \dot{q}^+ \\ F_c \end{bmatrix} = \begin{bmatrix} M_r\dot{q}^- \\ -e\Xi_6\dot{q}^- \end{bmatrix} \quad (8)$$

After the heel-strike, the foot rotates around the ankle joint. The EoM of the model is:

$$\begin{bmatrix} M_r & \Xi_3^T & \Xi_6^T \\ \Xi_3 & 0 & 0 \\ \Xi_6 & 0 & 0 \end{bmatrix} \begin{bmatrix} \ddot{q} \\ F_{c1} \\ F_{c2} \end{bmatrix} = \begin{bmatrix} F_r \\ -\tilde{\Xi}_3 \\ -\tilde{\Xi}_6 \end{bmatrix} \quad (9)$$

Note that the constraint equations guarantee that the stance leg maintains foot contact with ground and the swing leg maintains heel contact with ground. In addition, the spring constant k in the compliant ankle joints should not be too big. Otherwise, the stance leg will lose contact with ground. In this phase, since the foot rotates around the ankle joint, the force generated by the springs on the swing leg should be considered as external force. Thus, in this event, the mass matrix M would not include the point mass of the swing foot.

2.4 Toe-strike Impulse

The proposed walking model with flat feet introduces a toe-strike impulse in addition to the heel-strike collision. The EoM of the model is:

$$\begin{bmatrix} M_r & \Xi_4^T \\ \Xi_4 & 0 \end{bmatrix} \begin{bmatrix} \dot{q}^+ \\ F_c \end{bmatrix} = \begin{bmatrix} M_r\dot{q}^- \\ -e\Xi_4\dot{q}^- \end{bmatrix} \quad (10)$$

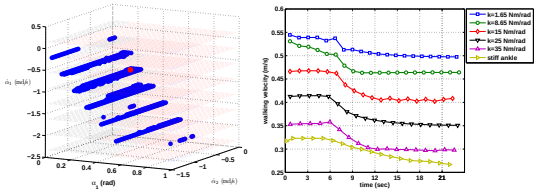

(a) (b)

Figure 2: (a) Basin of attraction of the passive dynamic walking model with flat feet and compliant ankles. The blue layers of points represent horizontal slices of a three-dimensional region of initial conditions that eventually result in the cyclic walking motion. The fixed point is indicated with a red point, which is above one of the sample slices. (b) Results of actively changing walking speed with the same hip actuation and different ankle compliance (k varies).

Note that in this phase, we consider that the ankle joint of the swing leg is constrained to move in a circular orbit with toe as the center and distance between toe and ankle joint as the radius. The force generated by the spring on the swing leg should be considered as external force, which can also be considered as the constraint force of the circular orbit. After the toe-strike, one step ends.

2.5 Effects of Hip Actuation and Ankle Compliance

By application of the cell mapping method that has been used in the several studies of passive dynamic walking (e.g. (Wisse et al., 2004), (Wisse et al., 2007)), we found that the model performs well in the concept of global stability. The allowable errors can be much larger than the results obtained in (Wisse et al., 2004). This can be inspected by the evaluation of the basin of attraction as shown in Fig. 2(a), which is the complete set of initial conditions that eventually result in cyclic walking motion. One can find that cyclic walking with initial conditions in Table 1, emerges even if the initial step is nearly fourfold as large, e.g. $\{\alpha_1(0) = 0.8, \dot{\alpha}_1(0) = -2.3, \dot{\alpha}_2(0) = -0.8\}$. It indicates that passive dynamic walking with flat feet and ankle compliance may play better on rough terrain with ground disturbance.

It has been examined that optimized hip actuation can improve the stability of the passive walker (Kurz and Stergiou, 2005). In addition, one can use the hip actuation as the control parameter to achieve stable walking on uneven terrain (Schuitema et al., 2005)-(Ueno et al., 2006). In our model mentioned above, ankle compliance k can also be used as a control parameter to affect the walking gait. As shown in Fig. 2(b), under the same change of hip actuation, different ankle compliance reveals different responses in walking velocity transition. It indicates that more compliance results in more visible sensitivity to the change of hip torque. According to the analysis of basins of attraction with different k (Wang et al., 2007), we find that a relatively small k will lead to more stable points. However, more compliance in ankle joints may result in often falling backward during walking. Thus, optimized ankle compliance may result in a more stable bipedal walking that allows larger disturbance.

3 OPTIMIZATION BASED WALKING CONTROL

In order to optimize the hip actuation and ankle compliance which affect walking gait as analyzed above, Particle Swarm Optimization (PSO) has been chosen with a focus lying on quickly finding suitable results, in view of time-consuming and adaptivity of the gait. In the realization of the PSO algorithm, a swarm of N particles is constructed inside a D-dimensional real valued solution space, where each position can be a potential solution for the optimization problem. The position of each particle is denoted as X_i $(0 < i < N)$. Each particle has a velocity parameter V_i $(0 < i < N)$. It specifies that the length and the direction of X_i should be modified during iteration. A fitness value attached to each location represents how well the location suits the optimization problem. The fitness value can be calculated by a fitness function of the optimization.

In this study, we used adaptive PSO with changing inertia weight. The update equation for velocity with inertial weight is described as follows:

$$v_{id}^{k+1} = w v_{id}^{k} + c_1 r_{1d}^{k}(pbest_{id}^{k} - x_{id}^{k}) + c_2 r_{2d}^{k}(gbest_{d}^{k} - x_{id}^{k}) \quad (11)$$

where w is the inertia weight. v_{id}^{k} is one component of V_i (d donates the component number) at iteration k. Similarly, x_{id}^{k} is one component of X_i at iteration k. $pbest_i$ $(0 < i < N)$ and $gbest$ are the personal best position and the global best position at each iteration respectively. c_1 and c_2 are acceleration factors. r_1 and r_2 are random numbers uniformly distributed between 0 and 1. Note that each component of the velocity has new random numbers. In order to prevent particles from flying outside the searching space, the amplitude of the velocity is constrained inside a spectrum $[-v_d^{max}, +v_d^{max}]$.

3.1 Fitness Function and Optimization Process

For a specific passive walker, the mechanical parameters (length and mass distribution) are constant. To control passive dynamic walking on uneven terrain, we focus the control parameters on hip actuation P and ankle compliance k. Then the two-dimensional parameter space is $(P,\ k)$. Here a set of parameters stands for a particle of PSO. Since the walker will be optimized with integration of stability and efficiency, the fitness function is defined as follows:

$$\sigma = \sigma_s + \gamma\sigma_e \tag{12}$$

where σ_s and σ_e are the fitness value to assess the stability and efficiency of each set of parameters respectively. γ is the tuning factor to change the importance of the two characteristics.

There are several methods to evaluate the stability of the passive dynamic walking. In this study, the stability will be quantified by the modulus of the Jacobian matrix of the mapping function as defined in (Wisse et al., 2004). Here, we notate the maximal eigenvalue as λ_m, which represents the decreasing speed of the deviation. The stability grades varies for different sets of parameters even they all have a stable fixed point. The smaller the λ_m is, the faster the deviation decreases and the more stable the walker is. The similar conclusion can be obtained when all sets of parameters only have an unstable fixed point. The larger the λ_m is, the more far from the stable state the walker is. Then we define the fitness function of stability as the follows:

$$\sigma_s = \frac{1}{\lambda_m} \tag{13}$$

Similar to (Collins et al. 2005) and (Wisse et al., 2004), the energetic efficiency of walking can be evaluated by the specific resistance as follows:

$$\Theta = \frac{E}{MgL} \tag{14}$$

where E is the cost of energy. In this study, the energy cost is generated only by the hip torque. M is the total mass of the model. g is the acceleration of gravity. L is the length of distance the robot passed. Then the fitness function can be defined as follows:

$$\sigma_e = \frac{1}{\Theta} = \frac{Mgl}{E} \tag{15}$$

From (12), (13) and (15), we can obtain the whole expression of the fitness function:

$$\sigma = \frac{1}{\lambda_m} + \gamma\frac{Mgl}{E} \tag{16}$$

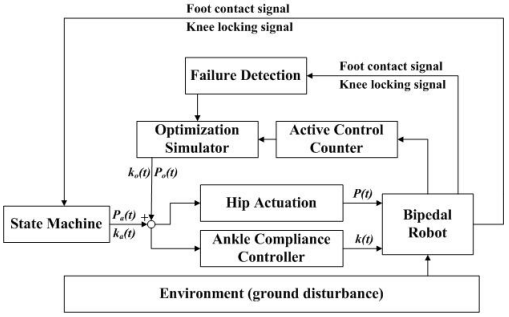

Figure 3: The control scheme to overcome ground disturbance with optimized hip torque and ankle compliance.

Additionally, to evaluate the walking motion after overcoming ground disturbance, we introduce another expression of fitness function. We use further walking distance d instead of the fitness efficiency σ_e. Then the fitness function can be rewritten as:

$$\sigma = \frac{1}{\lambda_m} + \gamma d \tag{17}$$

3.2 Gait Controller with Optimized Parameters

After analyzing the effects of hip actuation and ankle compliance in the stability and adaptability of the passive dynamic walker, we select P and k as the gait control input. The output of the optimization simulator $P_o(t)$ and $k_o(t)$ are added to the current actual hip actuation $P_a(t)$ and ankle compliance $k_a(t)$ (see Fig. 3).

This results in extra hip torque to move the swing leg more forward and prevent tripping. The purpose of the failure-detection block in Fig. 3 is to monitor in simulations the foot contact and the knee locking in order to detect whether walking failed. A failure means that the robot fell either backward or forward or that it started running (both feet leave contact with ground). There is a active control counter module in the diagram. It is used to count the times of applying active control (increasing or decreasing P or k) during one continuous walking. The output of this module make the simulator change P or k. With the dynamic model that adequately describing the real robot, an adaptive optimizing control scheme can be done without manually set to teach the robot and without the robot damaging itself.

4 EXPERIMENTAL RESULTS

All the simulation experiments used the dynamic model mentioned in Section II which was imple-

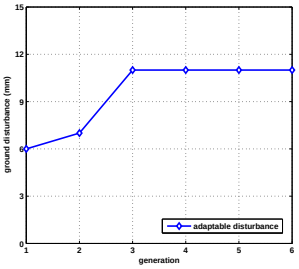

Figure 4: Maximum ground disturbance with optimized hip torque and ankle compliance that keep unchanged during stable walking.

mented in MATLAB, using the parameter values shown in Table 1. The numerical integration of the second order differential EoMs uses the Runge-Kutta method, which is similar to the simulation methods mentioned in (Wisse et al., 2004).

4.1 Parameter Optimization

Based on the adaptive PSO with proper inertial weight mentioned above, we optimized the hip torque (hip actuation) and ankle compliance to achieve adaptive walking with maximal allowable ground disturbance of the model with parameter values in Table 1. The testing scenario is a floor with one step down. The height of the step is gradually chosen from the range from $1mm$ to $20mm$. The initial particles which represent the parameter set of P and k are randomly selected from the corresponding points in 2(a) that will finally achieve stable walking. During the walking simulation of the dynamic model, the ground disturbance gradually increase. The optimization process evaluates the maximum ground disturbance of the dynamic model with certain P and k. During the walking, the selected P and k keep constant to overcome gradually increased ground disturbance. The optimization finally record the maximum ground disturbance in each generation. The fitness function is (16). Fig. 12 shows the results. It is clear that by applying the adaptive PSO, the optimization process can quickly find the optimal parameter set. It also indicated that with optimized hip actuation and ankle torque, the passive dynamic walker can achieve stable walking with no active control even if there is $-11mm$ ground disturbance.

4.2 Walking on Uneven Terrain with Control

Starting from the optimized P and k with no active control during walking simulations, we add the control scheme shown in Fig. 3 to the walking motion.

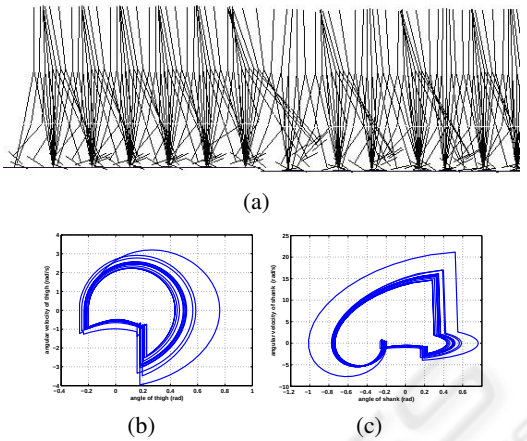

Figure 5: Adaptive locomotion with active control on uneven terrain. This result is obtained every 10 frames during a continuous walking. (a) is the stick diagram. (b) and (c) are the angular trajectories of the thigh and shank respectively.

A preset ground disturbance occurs at known time during the level walking. The active control counter determines the times of active control to change P and k. In this simulation, the ground disturbance varies from $-15mm$ to $-25mm$. The fitness function of the optimization is (17). The counter first makes the optimization simulator to actively change P and k once when ground disturbance occurs. There was no optimized set of P and k that can overcome the $-25mm$ step. Then the counter makes the simulator to actively change P and k twice when ground disturbance occurs. The walker successfully achieved stable walking with $-25mm$ disturbance (see stick diagram shown in Fig. 5(a)). Fig. 5(b) and (c) show the trajectories of hip and knee during the adaptive walking.

Note that the cyclic walking was initially actuated by a relatively small hip torque. After one time of active control (varying P and k), the hip torque increased to move the swing leg more forward and prevent tripping. Since there was a second time of active control, the trajectories of the swing thigh and the swing shank transited to bigger limit cycles. Such optimized P and k finally stabilized the walking motion after a step down occurred.

Fig. 6 shows the optimization process of the hip actuation and ankle compliance during the walking with two times of active control. We set that if the walker can walk stably for enough time after the ground disturbance, the walking motion is adaptive on the uneven ground. Specifically, the distance is the product of walking speed times 25 seconds. Fig. 6(a) demonstrates the results of further distance after ground disturbance each generation. After four gen-

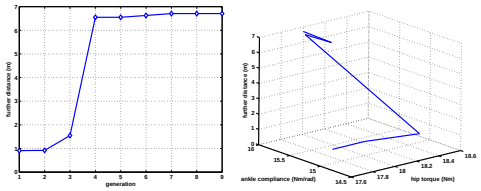

(a) (b)

Figure 6: Optimization of hip actuation and ankle compliance. Both P and k vary during the continuous walking. (a) is the results of further distance after ground disturbance each generation. (b) is the results of selecting hip actuation and ankle compliance during optimization.

erations, the walker can find optimized parameters to overcome the step. Fig. 6(b) shows the process of selecting P and k during the optimization. The initial hip torque is $5.5130Nm$ and ankle compliance is $12.2218Nm/rad$. The two times of variance of P and k are ($18.0000Nm$, $16.0000Nm/rad$ and ($5.5000Nm$, $15.4228Nm/rad$) respectively.

Though there is no complex learning algorithm in the control scheme, the walker can perform better terrain adaptability comparing with other simulation results (e.g. (Schuitema et al., 2005), (Wang et al., 2006)).

4.3 Real Robot Experiments

To study natural and energy-efficient bipedal walking, we designed and constructed a bipedal robot prototype, $1.2m$ in height and $20kg$ in weight. With the bisecting hip mechanism similar to (Wisse et al., 2007), the prototype has five Degrees of Freedom (DOFs). Two commercial motors are used in the hip joints to perform hip actuation. Each leg consists of a thigh and a shank interconnected through a passive knee joint that has a locking mechanism. Springs are installed between the foot and the plate that is pushing the leg up while it is rotated around the ankle. To prevent foot-scuffing, we modified the foot with arc in the front and the back-end. Specific mechanical parameters are shown in Table 1. In the experiment, by using the proposed method, the robot tried to walk on natural ground outdoor. The natural ground is not a strict continuous level floor, where random irregularity of the ground and slight slippery occurred. Fig. 7 shows the result.

The robot can achieve three-dimensional stable walking on natural ground with more than 10 steps. Comparing to the results of terrain adaptability of other real robot experiments (e.g. two-dimensional walkers (Wisse et al., 2005), (Ueno et al., 2006)), the successful three-dimensional walking of the robot prototype shows that the quasi-passive dynamic walker with optimized hip actuation and ankle compliance can perform stable walking with larger ground disturbance.

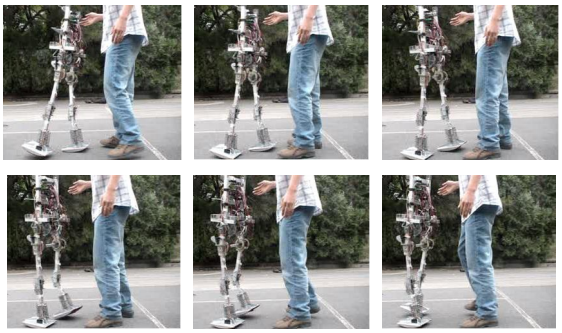

Figure 7: A sequence of photos captured during autonomous walking of the robot prototype on natural ground.

5 CONCLUSIONS

In this paper, we have investigated how to control passivity-based bipedal walkers to achieve stable locomotion with terrain adaptability. Satisfactory results of simulations and real robot experiments indicated that having the fixed mechanical parameters during walking, the passivity-based walker can walk on uneven terrain with larger ground disturbance by optimized hip actuation and ankle compliance in view of walking stability and efficiency. In the future, more real robot experiments will be continued to overcome more complex ground disturbance.

ACKNOWLEDGEMENTS

The authors would like to thank M. Wisse for sharing the simulation files of the simplest walking model. This work was supported by the National Natural Science Foundation of China (No. 60774089), National High Technology Research and Development Program of China (863 Program) (No. 2006AA04Z258) and 985 Project of Peking University.

REFERENCES

S. Collins, M. Wisse, A. Ruina, A three-dimensional passive-dynamic walking robot with two legs and knees, *International Journal of Robotics Research*, vol. 20, pp. 607-615, 2001.

S. Collins, A. Ruina, R. Tedrake, M. Wisse, Efficient bipedal robots based on passive-dynamic walkers, *Science*, vol. 307, pp. 1082-1085, 2005.

R. Eberhart, J. Kennedy, Particle swarm optimization, *Proc. of the IEEE Conf. on Neural Network*, 1995, pp. 1942-1948.

T. Fukunaga, K. Kubo, Y. Kawakami, S. Fukashiro, H. Kanehisa, C. N. Maganaris, In vivo behaviour of human muscle tendon during walking, *Proc. Biol. Sci.*, vol. 268, pp. 229-233, 2001.

M. Garcia, A. Chatterjee, A. Ruina, M. Coleman, The simplest walking model: stability, complexity, and scaling, *ASME Journal Biomechanical Engineering*, vol. 120: pp. 281–288, 1998.

Y. Guan, E. S. Neo, K. Yokoi, and K. Tanie, Stepping over obstacles with humanoid robots, *IEEE Transactions on Robotics*, **22**(5), pp. 958-973, 2006.

Honda Motor Co., Ltd. New asimo - running at 6km/h, http://world.honda.com/HDTV/ASIMO/New-ASIMO-run-6kmh/, 2005.

M. Kwan, M. Hubbard, Optimal foot shape for a passive dynamic biped, *Journal of Theoretical Biology*, vol. 248, pp. 331-339, 2007.

A. D. Kuo, Energetics of actively powered locomotion using the simplest walking model, *ASME Journal Biomechanical Engineering*, vol. 124, pp. 113-120, 2002.

M. J. Kurz, N. Stergiou, An artificial neural network that utilizes hip joint actuations to control bifurcations and chaos in a passive dynamic bipedal walking model, *Biol. Cybern.*, vol. 93, pp. 213-221, 2005.

T. McGeer, Passive dynamic walking, *International Journal of Robotics Research*, vol. 9, pp. 68-82, 1990.

P. Michel, J. Chestnutt, S. Kagami, K. Nishiwaki, J. Kuffner, and T. Kanade, GPU-accelerated real-time 3D tracking for humanoid locomotion and stair climbing, *Proc. of the IEEE/RSJ Int. Conf. on Intelligent Robots and Systems*, 2007, pp. 463–469.

A. Ruina, J. E. A. Bertram, M. Srinivasan, A collisional model of the energetic cost of support work qualitatively explains leg sequencing in walking and galloping, pseudo-elastic leg behavior in running and the walk-to-run transition, *Journal of Theoretical Biology*, vol. 237, no. 2, pp. 170-192, 2005.

E. Schuitema, D. Hobbelen, P. Jonker, M. Wisse, J. Karssen, Using a controller based on reinforcement learning for a passive dynamic walking robot, *Proc. of the IEEE-RAS Int. Conf. on Humanoid Robots*, 2005, pp. 232-237.

R. Smith, U. Rattanaprasert, and N. O'Dwyer, Coordination of the ankle joint complex during walking, *Huamn Movement Science*, vol. 20, pp. 447-460, 2001.

R. Tedrake, T. W. Zhang, M. F. Fong, H. S. Seung, Actuating a Simple 3D Passive Dynamic Walker. In *Proc. IEEE Int. Conf. Robotics and Automation*, 2004, pp. 4656-4661.

T. Ueno, Y. Nakamura, T. Takuma, K. Hosoda, T. Shibata and S. Ishii, Fast and stable learning of quasi-passive dynamic walking by an unstable biped robot based on off-policy natural actor-critic, *Proc. of the IEEE/RSJ International Conference on Intelligent Robots and Systems*, 2006, pp. 5226-5231.

S. Wang, J. Braaksma, R. Babuška, D. Hobbelen, Reinforcement learning control for biped robot walking on uneven surfaces, *Proc. of the 2006 International Joint Conference on Neural Networks*, 2006, pp. 4173-4178.

Q. Wang, J. Zhu, L. Wang, Passivity-based three-dimensional bipedal robot with compliant legs, *Proc. of the SICE Annual Conference*, 2008.

M. Wisse, A. L. Schwab, F. C. T. Van der Helm, Passive dynamic walking model with upper body, *Robotica*, vol. 22, pp. 681-688, 2004.

M. Wisse, A. L. Schwab, R. Q. van der Linde, F. C. T. van der Helm, How to keep from falling forward: elementary swing leg action for passive dynamic walkers, *IEEE Transactions on Robotics*, vol. 21, no. 3, pp. 393-401, 2005.

M. Wisse, G. Feliksdal, J. van Frankenhuyzen, B. Moyer, Passive-based walking robot - Denise, a simple, efficient, and lightweight biped, *IEEE Robotics and Automation Magazine*, vol. 14, no. 2, pp. 52-62, 2007.

J. Yamaguchi and A. Takanishi, Development of a leg part of a humanoid robot - development of a biped walking robot adapting to the humans' normal living floor, *Autonomous Robots* 4(4), pp. 369-385, 1997.